Tran. Natl. Acad. Sci. Azerb. Ser. Phys.-Tech. Math. Sci.
Mechanics, **46** (7), 21–32 (2026);
https://doi.org/10.30546/2706-7734.46.7.2026.030

Impact of initial stretching stress in eccentric hollow cylinder on dispersion of waves propagating in cylinder

Sona S. Farajova

Received: 11.09.2025 / Revised: 24.12.2025 / Accepted: 05.04.2026

Abstract. *This paper studies the impact of initial stretching of an eccentric hollow cylinder on the dispersion of waves propagating within the cylinder. Three-dimensional linearized theory of elastic waves (TDLTEW) is used in bodies with initial stresses. To solve the corresponding eigenvalue problem, the method developed by the author in an earlier co-authored work is applied. This method uses Fourier series to transform expressions written in one cylindrical coordinate system into expressions in another cylindrical coordinate system, instead of using summation theorems for cylindrical functions. Until now, numerical results on the impact of cylinder eccentricity on wave dispersion have been obtained in the context of three-dimensional classical linear theory of elastodynamics only when there is no initial stretching in a cylinder. This paper attempts to extend these investigations to cases where the cylinder is initially stretched, using the TDLTEW in bodies with initial stresses. Numerical results on the impact of initial stretching in the cylinder on the dispersion curves are presented and discussed.*

Keywords. eccentric hollow cylinder · wave dispersion · initial stress · dispersion curves · Fourier series

Mathematics Subject Classification (2010): 74-10, 74B05, 74B10, 74E10

1 Introduction

To date, numerous studies have examined the dispersion of waves propagating in an initially stretched hollow cylinder whose central axis coincides with that of the cylindrical bore, i.e., coaxial hollow cylinders (see [1,4]).

However, corresponding investigations related to eccentric hollow cylinders are not so numerous. Such investigations are necessary because eccentric cylindrical components are widely used as basic structural elements in many engineering applications, such as machine

S.S. Farajova
Department of Mechanics, Baku State University, 23 Academician Z. Khalilov St., Baku AZ1148, Azerbaijan
E-mail: ferecovasona97@gmail.com

parts, gun barrels, and pipes (see [8, 9] for examples). Nevertheless, only a few investigations (see [2, 5–7]) have been made until now on dynamics of the eccentric hollow cylinder using the three-dimensional exact equations of linear elastodynamics, which cannot take into consideration the impact of initial stretching on the dynamics of eccentric hollow cylinder.

Note that in [7], the case of small eccentricity was considered. The main difficulty in solving the corresponding problems for eccentric cylinders is a satisfaction of boundary conditions on the eccentric cylindrical surfaces. In [7], where the distance between the central axis of the cylinder and the cylindrical bore is significantly smaller than the radius of the outer circle of the cylinder cross-section, this is achieved by applying the boundary form perturbation method. Numerical results are presented for the lowest frequencies under various values of problem parameters.

In [5], the natural frequencies of the eccentric hollow cylinder with finite length have been considered, while in [6] the vibroacoustic response of the infinite eccentric hollow cylinder embedded in an acoustic medium was treated. Both these papers use the summation theorem for Bessel functions to satisfy the boundary conditions.

Now about [2]. As in [5–7], this one treats the dispersion of waves in the eccentric hollow cylinder within the scope of three-dimensional linear elastodynamics. However, it develops a method where each term in the Fourier series, used to express the solutions of the field equations, is again represented as a Fourier series to satisfy the boundary conditions on the eccentric cylindrical surfaces. This method is based on the mentioned representation and differs from those of [5–7]. Furthermore, the paper [2] presents a lot of numerical results illustrating the impact of cylinder's eccentricity on the dispersion curves. This summarizes the research concerning the dynamics of the eccentric hollow cylinder. It follows from the foregoing discussion that, up to now, there have been no investigations on the dispersion of waves propagating in the eccentric cylinder with initial stresses.

In this paper, we make the first attempt in this field to investigate the corresponding problem within the scope of TDLTEW in bodies with initial stresses, using the method developed in [2]. Numerical results on the impact of initial stresses on wave dispersion in the eccentric cylinder are presented and analyzed.

2 Problem statement and solution method

Consider a circular cylinder of infinite length and assume that this cylinder contains an eccentric cylindrical hole also of infinite length (Fig. 2a). Assume that the central axes of the cylinder and the cylindrical hole are parallel to each other and that the distance between these axes is R_{cb}. We associate the coordinates in cylindrical system $Or\theta z$ with those in Cartesian system $Ox_1x_2x_3$ by means of the central axis of the cylinder. Moreover, we assume that $z = x_3$, the center of the cylindrical hole is on the coordinate axis Ox_1, and the distance between this center and the chosen origin of the coordinate system is R_{cb}.

We also assume that the cross-section of this hole is a circle of radius R_b. At the same time, we suppose that the cross-section of the cylinder is a double-connected eccentric circle which occupies some part of the circle of radius R_c ($R_c > R_b$), from which a circle of radius R_b is subtracted (Fig. 2b). We also associate the Cartesian coordinate system $O_0x_{10}x_{20}x_{30}$ with the cylindrical coordinate system $O_0r_0\theta_0z_0$ by means of the central axis of the cylindrical hole. The relationship between these two coordinate systems is as follows:

$$\begin{gathered} x_1 = R_{cb} + x_{10}, \qquad x_2 = x_{20}, \qquad x_3 = x_{30}, \\ r\exp(i\theta) = R_{cb} + r_0\exp(i\theta_0), \qquad z = z_0. \end{gathered} \tag{2.1}$$

Following the above preparatory procedure, in accordance with [1, 4], we derive the field equations of the three-dimensional linearized theory of elastic waves in bodies with initial

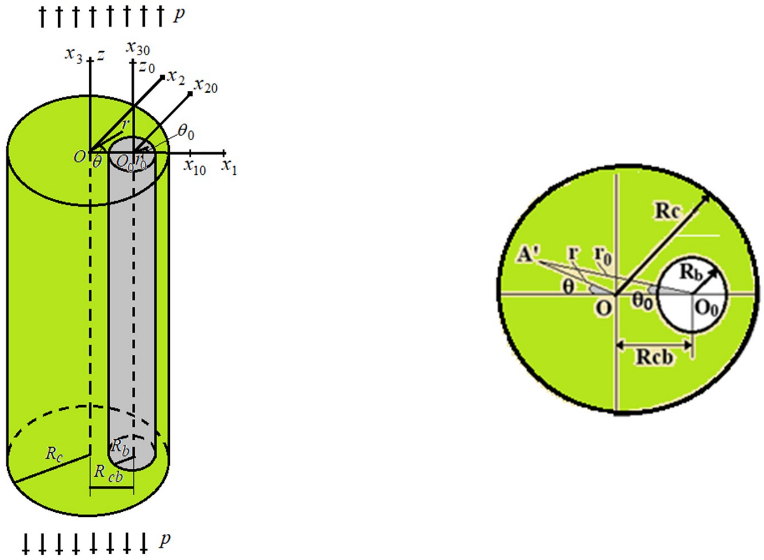

a b

Fig.2.1. The sketch of the initially stretched eccentric hollow cylinder, selected coordinate systems (a), and the geometry of the cross section of this cylinder (b).

stresses in the cylindrical coordinate system in case where the material of the cylinder is isotropic and homogeneous.

The equations of motion are as follows:

$$\begin{aligned}
&\frac{\partial\sigma_{rr}}{\partial r}+\frac{1}{r}\frac{\partial\sigma_{r\theta}}{\partial\theta}+\frac{\partial\sigma_{rz}}{\partial z}+\frac{\sigma_{rr}-\sigma_{\theta\theta}}{r}+\sigma_{zz}^{0}\frac{\partial^2u_r}{\partial z^2}=\rho\frac{\partial^2u_r}{\partial t^2},\\
&\frac{\partial\sigma_{\theta r}}{\partial r}+\frac{1}{r}\frac{\partial\sigma_{\theta\theta}}{\partial\theta}+\frac{\partial\sigma_{\theta z}}{\partial z}+\frac{2}{r}\sigma_{\theta r}+\sigma_{zz}^{0}\frac{\partial^2u_\theta}{\partial z^2}=\rho\frac{\partial^2u_\theta}{\partial t^2},\\
&\frac{\partial\sigma_{zr}}{\partial r}+\frac{1}{r}\frac{\partial\sigma_{z\theta}}{\partial\theta}+\frac{\partial\sigma_{zz}}{\partial z}+\frac{1}{r}\sigma_{zr}+\sigma_{zz}^{0}\frac{\partial^2u_z}{\partial z^2}=\rho\frac{\partial^2u_z}{\partial t^2}.
\end{aligned}\tag{2.2}$$

Elasticity relations:

$$\begin{aligned}
&\sigma_{rr}=\lambda(\varepsilon_{rr}+\varepsilon_{\theta\theta}+\varepsilon_{zz})+2\mu\varepsilon_{rr},\\
&\sigma_{\theta\theta}=\lambda(\varepsilon_{rr}+\varepsilon_{\theta\theta}+\varepsilon_{zz})+2\mu\varepsilon_{\theta\theta},\\
&\sigma_{zz}=\lambda(\varepsilon_{rr}+\varepsilon_{\theta\theta}+\varepsilon_{zz})+2\mu\varepsilon_{zz},\\
&\sigma_{\theta z}=2\mu\varepsilon_{\theta z},\qquad \sigma_{rz}=2\mu\varepsilon_{rz},\qquad \sigma_{r\theta}=2\mu\varepsilon_{r\theta}.
\end{aligned}\tag{2.3}$$

Strain-displacement relations:

$$\begin{aligned}
&\varepsilon_{rr}=\frac{\partial u_r}{\partial r},\qquad \varepsilon_{\theta\theta}=\frac{u_r}{r}+\frac{1}{r}\frac{\partial u_\theta}{\partial\theta},\qquad \varepsilon_{zz}=\frac{\partial u_z}{\partial z},\\
&\varepsilon_{r\theta}=\frac{1}{2}\left(\frac{\partial u_r}{r\partial\theta}+\frac{\partial u_\theta}{\partial r}-\frac{u_\theta}{r}\right),\quad \varepsilon_{\theta z}=\frac{1}{2}\left(\frac{\partial u_z}{r\partial\theta}+\frac{\partial u_\theta}{\partial z}\right),\quad \varepsilon_{rz}=\frac{1}{2}\left(\frac{\partial u_r}{\partial z}+\frac{\partial u_z}{\partial r}\right).
\end{aligned}\tag{2.4}$$

The system of equations (2.2)–(2.4) must be provided with various boundary and initial conditions that relate to the type of specific dynamic problem under consideration. For example, if the dispersion of the waves propagating in the cylinder in the direction of the

Oz axis is considered, then the following boundary conditions can be imposed at $r = R_c$ and $r_0 = R_b$:

$$\begin{aligned} &\sigma_{rr}|_{r=R_c} = 0, \qquad \sigma_{r\theta}|_{r=R_c} = 0, \qquad \sigma_{rz}|_{r=R_c} = 0, \\ &\sigma_{rr}|_{r_0=R_b} = 0, \qquad \sigma_{r\theta}|_{r_0=R_b} = 0, \qquad \sigma_{rz}|_{r_0=R_b} = 0. \end{aligned} \tag{2.5}$$

This completes the problem statement.

Now, following [2], let us consider the solution method for our problem. First, note that the method to be discussed below was not only presented in [2] for the case where initial stresses are absent in the cylinder, but was also briefly reported at the 9th International Conference on Control and Optimization with Industrial Applications, August 27–29, 2024, Istanbul, Turkey [3] for the case where the cylinder has homogeneous initial stresses. However, in [3], no numerical results on the impact of initial stresses on the dispersion curves were stated.

Let us introduce the potentials Ψ and X [4]. Then the displacements are described as follows:

$$\begin{aligned} u_r &= \frac{\partial \Psi}{r\partial\theta} - \frac{\partial^2 X}{\partial r \partial z}, \\ u_\theta &= -\frac{\partial \Psi}{\partial r} - \frac{\partial^2 X}{r\partial\theta\partial z}, \\ u_z &= (A_{13} + A_{44})^{-1} \left(A_{11}\Delta_1 + A_{44}\frac{\partial^2}{\partial z^2} - \rho\frac{\partial^2}{\partial t^2} \right) X, \\ \Delta_1 &= \frac{\partial^2}{\partial r^2} + \frac{1}{r}\frac{\partial}{\partial r} + \frac{1}{r^2}\frac{\partial^2}{\partial \theta^2}. \end{aligned} \tag{2.6}$$

The potentials satisfy the equations

$$\begin{aligned} &\left(\Delta_1 + \xi_1^2 \frac{\partial^2}{\partial z^2} - \frac{\rho}{2\mu}\frac{\partial^2}{\partial t^2} \right) \Psi = 0, \\ &\left\{ \left(\Delta_1 + \xi_2^2 \frac{\partial^2}{\partial z^2} \right) \left(\Delta_1 + \xi_3^2 \frac{\partial^2}{\partial z^2} \right) - \rho \left(\frac{\lambda + 3\mu}{(\lambda+2\mu)\mu}\Delta_1 + \frac{\lambda + 3\mu + 2\sigma_{zz}^0}{(\lambda+2\mu)\mu}\frac{\partial^2}{\partial z^2} \right) \frac{\partial^2}{\partial t^2} \right. \\ &\qquad \left. + \frac{\rho^2}{(\lambda+2\mu)\mu}\frac{\partial^4}{\partial t^4} \right\} X = 0. \end{aligned} \tag{2.7}$$

According to [4], the constants ξ_1, ξ_2, and ξ_3 are defined by

$$\begin{aligned} \xi_1^2 &= \frac{\mu + \sigma_{33}^0}{2\mu}, \\ \xi_{2,3}^2 &= c \pm \left[c^2 - \frac{((\lambda+2\mu) + \sigma_{33}^0)(\mu + \sigma_{33}^0)}{(\lambda+2\mu)\mu} \right]^{1/2}, \\ 2(\lambda+2\mu)\mu c &= (\lambda+2\mu)((\lambda+2\mu) + \sigma_{33}^0) + \mu(\mu + \sigma_{33}^0) - (\lambda+\mu)^2. \end{aligned} \tag{2.8}$$

Expressing the potentials Ψ and X as

$$\begin{aligned} \Psi &= \cos(kz - \omega t) \sum_{n=-\infty}^{+\infty} \Psi_n^0(r_0) e^{in\theta_0}, \quad \Psi_n^0(r_0) = \Psi_{1n}^0(r_0) + \Psi_{2n}^0(r_0), \\ X &= \sin(kz - \omega t) \sum_{n=-\infty}^{+\infty} X_n^0(r_0) e^{in\theta_0}, \quad X_n^0(r_0) = X_{1n}^0(r_0) + X_{2n}^0(r_0), \end{aligned} \tag{2.9}$$

and substituting these expressions into (2.7), we derive the following equations for the functions $\Psi_n^0(r_0)$ and $X_n^0(r_0)$:

$$\left(\Delta_{1n}^0+\zeta_1^2\right)\Psi_n^0=0,\ \left(\Delta_{1n}^0+\zeta_2^2\right)\left(\Delta_{1n}^0+\zeta_3^2\right)X_n^0=0, \Delta_{1n}^0=\frac{\partial^2}{\partial r_0^2}+\frac{1}{r_0}\frac{\partial}{\partial r_0}-\frac{n^2}{r_0^2}. \quad (2.10)$$

Here

$$\zeta_1^2=k^2(2\mu/2)^{-1}\left(\rho c^2-(\mu+\sigma_{33}^0)\right), \quad (2.11)$$

and ζ_2^2 and ζ_3^2, according to [4], are obtained from the following equation:

$$\begin{aligned}(\lambda+2\mu)\mu\zeta^4-k^2\zeta^2\Big[&(\lambda+2\mu)(\rho c^2-(\lambda+2\mu)-\sigma_{33}^0)\\&+A_{44}(\rho c^2-\mu-\sigma_{33}^0)+(\lambda+\mu)^2\Big]\\&+k^4(\rho c^2-(\lambda+2\mu)-\sigma_{33}^0)(\rho c^2-\mu-\sigma_{33}^0)=0.\end{aligned} \quad (2.12)$$

We obtain the solutions to the equations in (2.10) as follows:

$$\begin{aligned}&\Psi_{1n}^0=\begin{cases}B_{1n}J_n(\zeta_1 kr_0), & \zeta_1^2>0,\\ B_{1n}I_n(\zeta_1 kr_0), & \zeta_1^2<0,\end{cases} \qquad \Psi_{2n}^0=\begin{cases}C_{1n}Y_n(\zeta_1 kr_0), & \zeta_1^2>0,\\ C_{1n}K_n(\zeta_1 kr_0), & \zeta_1^2<0,\end{cases}\\ &X_{1n}^0=\begin{cases}B_{2n}J_n(\zeta_2 kr_0), & \zeta_2^2>0,\\ B_{2n}I_n(\zeta_2 kr_0), & \zeta_2^2<0,\end{cases}\\ &\qquad+\begin{cases}B_{3n}J_n(\zeta_3 kr_0), & \zeta_3^2>0,\\ B_{3n}I_n(\zeta_3 kr_0), & \zeta_3^2<0,\end{cases}\\ &X_{2n}^0=\begin{cases}C_{2n}Y_n(\zeta_2 kr_0), & \zeta_2^2>0,\\ C_{2n}K_n(\zeta_2 kr_0), & \zeta_2^2<0,\end{cases}\\ &\qquad+\begin{cases}C_{3n}Y_n(\zeta_3 kr_0), & \zeta_3^2>0,\\ C_{3n}K_n(\zeta_3 kr_0), & \zeta_3^2<0.\end{cases}\end{aligned} \quad (2.13)$$

Here $J_n(x)$ and $Y_n(x)$ ($I_n(x)$ and $K_n(x)$) are the n-th order Bessel functions (modified Bessel functions) of the first and second kinds.

Using the solutions (2.13) and expressions (2.6), (2.4), and (2.3), we obtain the expressions for the displacements and stresses in the form of infinite series, similar to the series (2.9). We can formally represent these series as follows:

$$\begin{aligned}\sigma_{rr}=\cos(kz-\omega t)\sum_{n=0}^{\infty}\big[&B_{1n}\sigma_{rrn1}(r_0)+B_{2n}\sigma_{rrn2}(r_0)+B_{3n}\sigma_{rrn3}(r_0)\\&+C_{1n}\sigma_{rrn4}(r_0)+C_{2n}\sigma_{rrn5}(r_0)+C_{3n}\sigma_{rrn6}(r_0)\big]e^{in\theta_0},\\ \sigma_{r\theta}=\cos(kz-\omega t)\sum_{n=0}^{\infty}\big[&B_{1n}\sigma_{r\theta n1}(r_0)+B_{2n}\sigma_{r\theta n2}(r_0)+B_{3n}\sigma_{r\theta n3}(r_0)\\&+C_{1n}\sigma_{r\theta n4}(r_0)+C_{2n}\sigma_{r\theta n5}(r_0)+C_{3n}\sigma_{r\theta n6}(r_0)\big]e^{in\theta_0},\\ \sigma_{rz}=\sin(kz-\omega t)\sum_{n=0}^{\infty}\big[&B_{1n}\sigma_{rzn1}(r_0)+B_{2n}\sigma_{rzn2}(r_0)+B_{3n}\sigma_{rzn3}(r_0)\\&+C_{1n}\sigma_{rzn4}(r_0)+C_{2n}\sigma_{rzn5}(r_0)+C_{3n}\sigma_{rzn6}(r_0)\big]e^{in\theta_0}.\end{aligned} \quad (2.14)$$

Here $B_{1n}, B_{2n}, B_{3n}, C_{1n}, C_{2n}$, and C_{3n} are the unknown constants, while the functions $\sigma_{rrn1}(r_0), \sigma_{rrn2}(r_0), \ldots, \sigma_{rzn5}(r_0), \sigma_{rzn6}(r_0)$ are the known ones. The explicit expressions for these functions are not given here to reduce the volume of the paper.

Now we try to satisfy the boundary conditions (2.5). First, let us consider the satisfaction of boundary conditions on the surface of the cylindrical bore. Using (2.14), we obtain the following system of linear algebraic equations for the unknown constants B_{1n}, B_{2n}, B_{3n}, C_{1n}, C_{2n}, and C_{3n}. Equating to zero the coefficients of $e^{in\theta_0}$, we obtain an infinite number of equations for the above-mentioned unknown coefficients.

Let us now consider the satisfaction of boundary conditions at the external surface of the cylinder, i.e., at $r = R_c$ (Fig. 2). For the satisfaction of these conditions, the expressions in (2.14) must be rewritten in the cylindrical coordinate system $Or\theta z$, i.e., in terms of the coordinates r and θ. Note that this rewriting can be made by using the summation theorem for cylindrical functions. However, it may also be made by using the Fourier series presentation for expressions (2.14) with respect to $e^{in\theta}$. In this work, we prefer the latter approach for the satisfaction of boundary conditions at $r = R_c$. For this purpose, we use the expressions

$$\begin{aligned} r_0 &= R_c\sqrt{1 - 2\frac{R_{cb}}{R_c}\cos\theta + \left(\frac{R_{cb}}{R_c}\right)^2}, \\ \cos(n\theta_0) &= \mathrm{Re}\left[\left(e^{i\theta} - \frac{R_{cb}}{R_c}\right)^n \left(1 - 2\frac{R_{cb}}{R_c}\cos\theta + \left(\frac{R_{cb}}{R_c}\right)^2\right)^{-n/2}\right], \\ \sin(n\theta_0) &= \mathrm{Im}\left[\left(e^{i\theta} - \frac{R_{cb}}{R_c}\right)^n \left(1 - 2\frac{R_{cb}}{R_c}\cos\theta + \left(\frac{R_{cb}}{R_c}\right)^2\right)^{-n/2}\right]. \end{aligned} \tag{2.15}$$

These are the equations of the $r = R_c$ surface in the coordinate system $O_0r_0\theta_0z_0$. Thus, substituting expressions (2.15) for the coordinates r_0 and θ_0 into (2.14), we obtain

$$\begin{aligned} \sigma_{rr}|_{r=R_c} &= \cos(kz - \omega t)\sum_{n=0}^{\infty}\Big[B_{1n}\sigma_{rrn1}(r_0(R_c,\theta)) + B_{2n}\sigma_{rrn2}(r_0(R_c,\theta)) \\ &\quad + B_{3n}\sigma_{rrn3}(r_0(R_c,\theta)) + C_{1n}\sigma_{rrn4}(r_0(R_c,\theta)) + C_{2n}\sigma_{rrn5}(r_0(R_c,\theta)) \\ &\quad + C_{3n}\sigma_{rrn6}(r_0(R_c,\theta))\Big]e^{in\theta_0(R_c,\theta)} = 0, \\ \sigma_{r\theta}|_{r=R_c} &= \cos(kz - \omega t)\sum_{n=0}^{\infty}\Big[B_{1n}\sigma_{r\theta n1}(r_0(R_c,\theta)) + B_{2n}\sigma_{r\theta n2}(r_0(R_c,\theta)) \\ &\quad + B_{3n}\sigma_{r\theta n3}(r_0(R_c,\theta)) + C_{1n}\sigma_{r\theta n4}(r_0(R_c,\theta)) + C_{2n}\sigma_{r\theta n5}(r_0(R_c,\theta)) \\ &\quad + C_{3n}\sigma_{r\theta n6}(r_0(R_c,\theta))\Big]e^{in\theta_0(R_c,\theta)} = 0, \\ \sigma_{rz}|_{r=R_c} &= \cos(kz - \omega t)\sum_{n=0}^{\infty}\Big[B_{1n}\sigma_{rzn1}(r_0(R_c,\theta)) + B_{2n}\sigma_{rzn2}(r_0(R_c,\theta)) \\ &\quad + B_{3n}\sigma_{rzn3}(r_0(R_c,\theta)) + C_{1n}\sigma_{rzn4}(r_0(R_c,\theta)) + C_{2n}\sigma_{rzn5}(r_0(R_c,\theta)) \\ &\quad + C_{3n}\sigma_{rzn6}(r_0(R_c,\theta))\Big]e^{in\theta_0(R_c,\theta)} = 0. \end{aligned} \tag{2.16}$$

We expand these expressions to the Fourier series with respect to $e^{in\theta}$ as follows:

$$\begin{gathered}
\sigma_{rrnj}(\zeta_j k r_0(R_c,\theta))e^{in\theta_0(R_c,\theta)} = \sum_{k=0}^{\infty}\sigma_{rrnjk}(\zeta_j k R_c)e^{ik\theta}, \qquad j=1,2,\ldots,6,\\
\sigma_{r\theta nj}(\zeta_j k r_0(R_c,\theta))e^{in\theta_0(R_c,\theta)} = \sum_{k=0}^{\infty}\sigma_{r\theta njk}(\zeta_j k R_c)e^{ik\theta},\\
\sigma_{rznj}(\zeta_j k r_0(R_c,\theta))e^{in\theta_0(R_c,\theta)} = \sum_{k=0}^{\infty}\sigma_{rznjk}(\zeta_j k R_c)e^{ik\theta},\\
\sigma_{rrnjk}(\zeta_j k R_c) = \frac{1}{\pi}\int_{-\pi}^{+\pi}\sigma_{rrnj}(\zeta_j k r_0(R_c,\theta))e^{in\theta_0(R_c,\theta)}e^{ik\theta}\,d\theta,\\
\sigma_{r\theta njk}(\zeta_j k R_c) = \frac{1}{\pi}\int_{-\pi}^{+\pi}\sigma_{r\theta nj}(\zeta_j k r_0(R_c,\theta))e^{in\theta_0(R_c,\theta)}e^{ik\theta}\,d\theta,\\
\sigma_{rznjk}(\zeta_j k R_c) = \frac{1}{\pi}\int_{-\pi}^{+\pi}\sigma_{rznj}(\zeta_j k r_0(R_c,\theta))e^{in\theta_0(R_c,\theta)}e^{ik\theta}\,d\theta.
\end{gathered} \tag{2.17}$$

Thus, we obtain from (2.16) the following system of equations:

$$\begin{aligned}
\sigma_{rr}|_{r=R_c} = 0 \Rightarrow \sum_{k=0}^{\infty}\sum_{n=0}^{\infty}\big[&B_{1n}\sigma_{rrn1k} + B_{2n}\sigma_{rrn2k} + B_{3n}\sigma_{rrn3k}\\
&+ C_{1n}\sigma_{rrn4k} + C_{2n}\sigma_{rrn5k} + C_{3n}\sigma_{rrn6k}\big]e^{ik\theta} = 0,\\
\sigma_{r\theta}|_{r=R_c} = 0 \Rightarrow \sum_{k=0}^{\infty}\sum_{n=0}^{\infty}\big[&B_{1n}\sigma_{r\theta n1k} + B_{2n}\sigma_{r\theta n2k} + B_{3n}\sigma_{r\theta n3k}\\
&+ C_{1n}\sigma_{r\theta n4k} + C_{2n}\sigma_{r\theta n5k} + C_{3n}\sigma_{r\theta n6k}\big]e^{ik\theta} = 0,\\
\sigma_{rz}|_{r=R_c} = 0 \Rightarrow \sum_{k=0}^{\infty}\sum_{n=0}^{\infty}\big[&B_{1n}\sigma_{rzn1k} + B_{2n}\sigma_{rzn2k} + B_{3n}\sigma_{rzn3k}\\
&+ C_{1n}\sigma_{rzn4k} + C_{2n}\sigma_{rzn5k} + C_{3n}\sigma_{rzn6k}\big]e^{ik\theta} = 0.
\end{aligned} \tag{2.18}$$

Thus, equating the coefficients of $e^{ik\theta}$ to zero, we obtain the second set of infinite system of linear equations for the unknown constants $B_{1n}, B_{2n}, B_{3n}, C_{1n}, C_{2n}$, and C_{3n}. In calculations, this infinite system is replaced by the corresponding finite system, i.e., it is assumed that

$$\sum_{k=0}^{\infty}\sum_{n=0}^{\infty}(\bullet) \approx \sum_{k=0}^{M}\sum_{n=0}^{N}(\bullet), \qquad M = N. \tag{2.19}$$

Combining this system with the one obtained from (2.15), we get the complete system of equations with respect to the above unknowns.

If we set the determinant of the coefficient matrix of this system equal to zero, then we obtain the corresponding dispersion equation. This equation can be formally stated as follows:

$$D = \det\left[\alpha_{qg}\left(\sigma_{zz}^0/\mu, c/c_2, kR_b, R_c/R_b, R_{cb}/R_c\right)\right] = 0, \qquad q,g = 1,2,\ldots,6N+4. \tag{2.20}$$

In case where $\sigma_{zz}^0/\mu = 0$, dispersion equation (2.20) coincides with the corresponding dispersion equation in [2].

Let us recall that the eccentricity of the cylinder is characterized by the ratio R_{cb}/R_c, where R_{cb} is the distance between the central axes of the cylinder and the cylindrical hole. If we assume $R_{cb}/R_c = 0$, then the determinant D is degenerate and the dispersion equation takes the following form:

$$D = D_{0(4\times4)}D_{1(6\times6)}D_{2(6\times6)}\cdots D_{N(6\times6)} = 0,$$

where $D_{0(4\times4)} = 0$ is a dispersion equation for the axisymmetric longitudinal waves in the corresponding coaxial hollow cylinder. However, the equation $D_{q(6\times6)} = 0$, $q = 1, 2, \ldots, N$, is a dispersion equation of the corresponding flexural wave of the q-th order propagating in the corresponding coaxial hollow cylinder.

In case where $R_{cb}/R_c > 0$, the determinant D does not degenerate, and to find the dispersion curves, dispersion equation (2.20) must be solved in its complicated form.

3 Numerical results and discussion

In this section, we present numerical results concerning the impact of initial stretching stress, that is $\sigma^0_{zz}/\mu > 0$, on the dispersion curves of longitudinal waves propagating in the eccentric hollow cylinder. Note that the testing of PC programs and algorithm used in this investigation is a direct extension of that used in [2]. Since the testing of this algorithm with the known results of [7] was already performed in [2], we do not consider this issue here again and proceed directly to the analysis of the results related to the impact of initial stress $\sigma^0_{zz}/\mu > 0$ on the dispersion curves of the lowest modes. It is known that the most significant impact of initial stresses on the dispersion curves is observed in these modes.

Let us consider specific numerical results obtained for a cylinder made of steel with Lamé constants $\lambda = 92.6$ GPa and $\mu = 77.5$ GPa, density $\rho = 7795$ kg/m^3, and shear wave propagation velocity $c_2 = 3153$ m/s. Assume $R_c/R_b = 1.5$ and $R_{cb}/R_c = 0.05$. Note that these numerical results (unless otherwise specified) are obtained when $M = N = 7$ in (2.19).

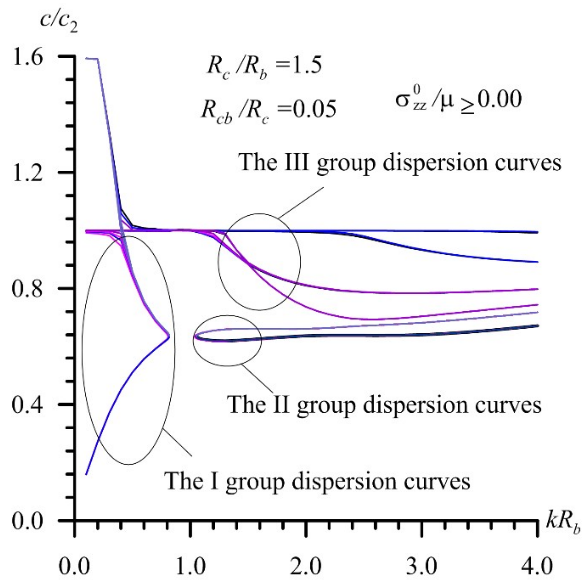

Fig.3.1. General view of the dispersion curves obtained for the lowest modes under various values of the initial stretching stress $\sigma^0_{zz}/\mu \geq 0$ for selected values of the problem parameters.

Now consider the dispersion curves in Fig. 3, which provide a general view of dispersion curves obtained for the lowest modes under various values of initial stress σ^0_{zz}/μ, using the problem parameters selected above. To simplify the discussion, we divide these curves into three groups as indicated in Fig. 3. It should be noted that when the initial stress is absent ($\sigma^0_{zz}/\mu = 0$), as in the case considered in [2], only two dispersion curves are obtained: one from group I and one from group II. Consequently, the dispersion curves in group III appear as a result of the presence of initial stretching stress.

We will analyze the dispersion curves in these groups separately. First, we consider the dispersion curves presented in Fig. 3, which illustrate the curves belonging to the first group.

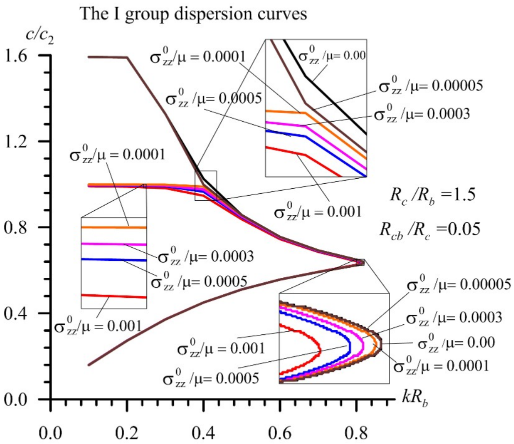

Fig.3.2. Dispersion curves of the I group constructed for various values of initial stress σ^0_{zz}/μ.

Figure 3 shows that the dispersion curves for the first group can be divided into two sections at the “return points”: those above the “return points” and those below them. Here, the “return point” refers to the point where $\partial(c/c_2)/\partial(kR_b) = \infty$. In Fig. 3, the dispersion curves around these points are magnified.

These graphs indicate that, as a result of initial stretching, the value of kR_b (denote it as $0 < kR_b \leq (kR_b)_{\mathrm{I}}$), at which $\partial(c/c_2)/\partial(kR_b) = \infty$, decreases as σ^0_{zz}/μ increases above zero. Furthermore, the graphs show that, due to initial stresses, the wave propagation velocity in the sections below (above) the “return points” increases (decreases) with the initial stretching of the cylinder. Figure 3 shows that the dispersion curves for the first group appear at $(kR_b)_{\mathrm{II}}; kR_b \geq (kR_b)_{\mathrm{II}}$ and $(kR_b)_{\mathrm{II}} > (kR_b)_{\mathrm{I}}$.

Moreover, the analysis of the dispersion curves for the first group shows that, in the sections above these curves, the wave propagation velocity approaches a limiting value as kR_b approaches zero. For $\sigma^0_{zz}/\mu \leq 0.00005$, this limit is approximately 1.6, while for $\sigma^0_{zz}/\mu \geq 0.0001$ it is approximately 1.0. This is a new and qualitative effect of initial stresses on the dispersion curves of waves propagating in the eccentric hollow cylinder.

Now let us consider the dispersion curves of the II group, shown in Fig. 3, which are constructed for various values of the initial stress σ^0_{zz}/μ. Figure 3 shows that these curves also have “return points” at their beginning. Denoting the values of kR_b at these “return points” by $(kR_b)_{\mathrm{return}}$, we see that the dispersion curves of the second group appear at $kR_b > 1$ and $(kR_b)_{\mathrm{return}} > 1$. These curves also indicate that the impact of the initial stress on the II group is not as significant as in the case of I group dispersion curves. Here, the initial stretching of the cylinder leads to a decrease in wave propagation velocity in the lower parts of these curves, but to an insignificant increase in wave propagation velocity in the upper parts. As above, “below” and “above” parts refer to the sections whose beginning points are below and above, respectively, the point at which $\partial(c/c_2)/\partial(kR_b) = \infty$. Thus,

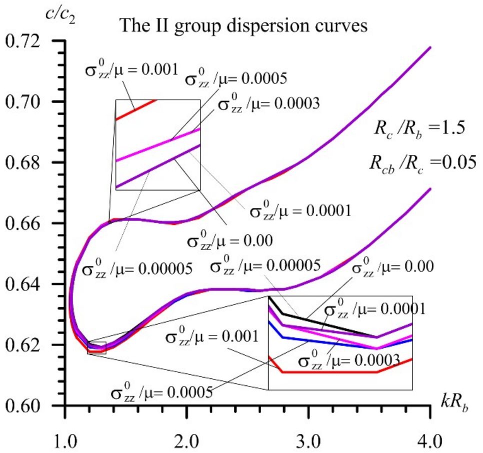

Fig.3.3. Dispersion curves of the II group constructed for various values of the initial stress σ^0_{zz}/μ.

the above discussion shows that the impact of the initial stress on the dispersion curves of the second group is only quantitative.

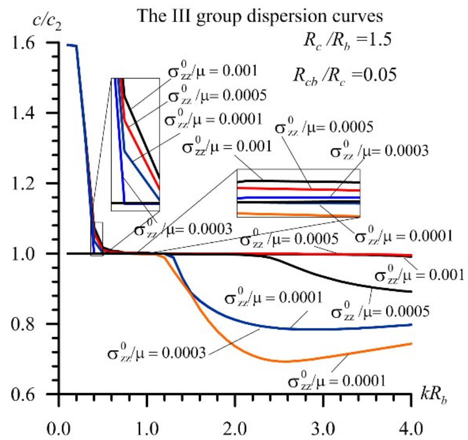

Fig.3.4. Dispersion curves of the III group constructed for various values of the initial stress σ^0_{zz}/μ.

Finally, let us consider the group III dispersion curves presented in Fig. 3. It should be noted that these curves arise specifically as a result of the initial stretching stress and may have several branches for a fixed value of the initial stress σ^0_{zz}/μ. For example, in cases where $\sigma^0_{zz}/\mu = 0.0001$ and 0.0005, the curves have two branches: one has a limiting wave propagation velocity approximately equal to 1.0, while the other is equal to 1.6 as kR_b approaches 0. The dispersion curves with the limiting value 1.6 are presumably the complementary corresponding dispersion curves of group I. Analysis of the group III dispersion curves shows that an increase in the values of the initial stress σ^0_{zz}/μ leads to an increase in the wave propagation velocity in the cases considered.

This completes the analysis of the results related to the impact of the initial stretching stress on the dispersion curves of waves propagating in the eccentric hollow cylinder.

Recall that all numerical results discussed above are obtained for the case where $M = N = 7$ in (2.19). To justify this choice of M and N, we consider results illustrating the convergence of these values. For this purpose, we refer to the graphs shown in Fig. 3, which are constructed for $\sigma^0_{zz}/\mu = 0.001$ for the I group dispersion curves. Figure 3 shows that

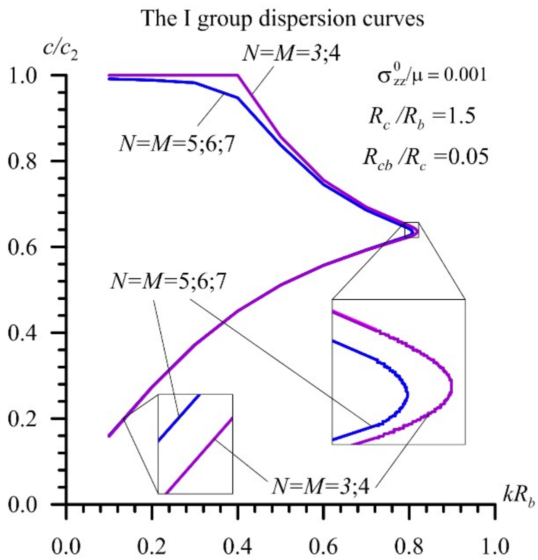

Fig.3.5. Convergence numerical results with respect to the values of $M = N$ in (2.19).

for $M = N = 5, 6$, and 7, the results almost completely coincide. This provides a certain guarantee of the reliability of the obtained and discussed results.

4 Conclusions

This paper deals with the impact of initial stretching of an eccentric hollow cylinder on the dispersion of waves propagating within the cylinder. The study was conducted using the three-dimensional linearized theory of elastic waves (TDLTEW) in bodies with initial stresses. To solve the corresponding eigenvalue problem, the method developed by the author in an earlier co-authored work is applied. This method uses Fourier series to transform expressions written in one cylindrical coordinate system into expressions in another cylindrical coordinate system, rather than using summation theorems for cylindrical functions. Until now, numerical results on the impact of cylinder eccentricity on wave dispersion have been obtained within the scope of the three-dimensional classical linear theory of elastodynamics only when there is no initial stretching of the cylinder. This paper attempts to extend these investigations to cases where the cylinder is initially stretched, using the TDLTEW in bodies with initial stresses. Numerical results on the impact of initial stretching of the cylinder on the dispersion curves are presented and discussed. According to the obtained results, it was established that, unlike in the coaxial hollow cylinder, the initial stresses in the eccentric hollow cylinder impact the dispersion curves not only quantitatively, but also qualitatively.

References

1. Akbarov, S. D. (2015). *Dynamics of pre-strained bi-material elastic systems: Linearized three-dimensional approach*. Springer. `https://doi.org/10.1007/978-3-319-14460-3`
2. Akbarov, S. D., & Farajova, S. S. (2025). The method for solving 3D problems of the eccentric hollow cylinder and its application to the study of wave dispersion propagating in this cylinder. *Structural Engineering and Mechanics, 96*(4), 257–270. `https://doi.org/10.12989/sem.2025.96.4.257`

3. Akbarov, S. D., Farajova, S. S., & Sevdimaliyev, Y. M. (2024). On the solution method of the dynamics of the eccentric hollow cylinder made of transversally isotropic material with homogeneous initial stresses. In *Proceedings of the 9th International Conference on Control and Optimization with Industrial Applications* (pp. 629–633). Istanbul, Turkey.
4. Guz, A. N. (2004). *Elastic waves in bodies with initial (residual) stresses*. A.C.K.
5. Hasheminejad, S. M., & Mirzaaei, Y. (2009). Free vibration analysis of an eccentric hollow cylinder using exact 3D elasticity theory. *Journal of Sound and Vibration, 326*, 687–702. https://doi.org/10.1016/j.jsv.2009.05.014
6. Hasheminejad, S. M., & Hessam, M.-A. (2012). Vibroacoustic response of an eccentric hollow cylinder. *Journal of Sound and Vibration, 331*, 3791–3808.
7. Shah, A. H. (1973). Elastic waves in a circular cylinder with an eccentric bore. *Acta Acustica united with Acustica, 28*(5), 251–258.
8. Tiersten, H. F., & Shick, D. V. (1995). Resonant wave propagation in gun tubes with eccentric bores. *Wave Motion, 21*, 75–84.
9. Wawk, V. (2000). *Machinery vibration*. McGraw-Hill.